

# Role of NH<sub>3</sub> in the Heterogeneous Formation of Secondary Inorganic Aerosols on Mineral Oxides

Weiwei Yang,<sup>†,‡,||</sup> Qingxin Ma,<sup>\*,†,‡,§</sup> Yongchun Liu,<sup>†,‡,§</sup> Jinzhu Ma,<sup>†,‡,§</sup> Biwu Chu,<sup>†,‡,§</sup> Ling Wang,<sup>†,‡</sup> and Hong He<sup>†,‡,§</sup>

<sup>†</sup>State Key Joint Laboratory of Environment Simulation and Pollution Control, Research Center for Eco-Environmental Sciences, Chinese Academy of Sciences, Beijing 100085, China

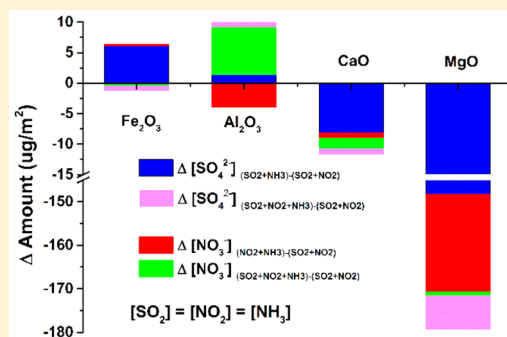
<sup>‡</sup>College of Resources and Environment, University of Chinese Academy of Sciences, Beijing 100049, China

<sup>§</sup>Center for Excellence in Urban Atmospheric Environment, Institute of Urban Environment, Chinese Academy of Sciences, Xiamen 361021, China

<sup>||</sup>Key Laboratory of Pesticide and Chemical Biology of Ministry of Education, Institute of Environmental and Applied Chemistry, College of Chemistry, Central China Normal University, Wuhan 430079, China

## Supporting Information

**ABSTRACT:** In this work, a relationship between the role of NH<sub>3</sub> and the properties of mineral oxides ( $\alpha$ -Fe<sub>2</sub>O<sub>3</sub>,  $\alpha$ -Al<sub>2</sub>O<sub>3</sub>, CaO, and MgO) in the evolution of NO<sub>3</sub><sup>-</sup>, SO<sub>4</sub><sup>2-</sup>, and NH<sub>4</sub><sup>+</sup> has been established. It was found that the promotion effect of NH<sub>3</sub> was more favorable for the formation of NO<sub>3</sub><sup>-</sup> (or SO<sub>4</sub><sup>2-</sup>) and NH<sub>4</sub><sup>+</sup> on acidic  $\alpha$ -Fe<sub>2</sub>O<sub>3</sub> and  $\alpha$ -Al<sub>2</sub>O<sub>3</sub> due to acid–base interactions between NO<sub>2</sub> with NH<sub>3</sub> or between SO<sub>2</sub> and NH<sub>3</sub>, while this effect was weaker on basic CaO and MgO possibly due to their basic nature. The acid–base interaction (NO<sub>2</sub>/SO<sub>2</sub> with NH<sub>3</sub>) overpowered the redox reaction (SO<sub>2</sub> with NO<sub>2</sub>) on Fe<sub>2</sub>O<sub>3</sub> owing to its unique redox chemistry. However, the opposite was found on basic CaO and MgO for the formation of SO<sub>4</sub><sup>2-</sup> and NO<sub>3</sub><sup>-</sup>. Under equivalent concentration conditions, the two synergistic effects did not further strengthen on Fe<sub>2</sub>O<sub>3</sub>, CaO and MgO due to a competition effect. In NH<sub>3</sub>-rich situation, a synchronous increase of SO<sub>4</sub><sup>2-</sup>, NO<sub>3</sub><sup>-</sup>, and NH<sub>4</sub><sup>+</sup> occurred on Fe<sub>2</sub>O<sub>3</sub>. On acidic Al<sub>2</sub>O<sub>3</sub>, the favorable adsorption of NH<sub>3</sub> on the surface as well as the existence of NO<sub>2</sub> with an oxidizing capability synergistically promoted the formation of SO<sub>4</sub><sup>2-</sup>, NO<sub>3</sub><sup>-</sup>, and NH<sub>4</sub><sup>+</sup>.



## 1. INTRODUCTION

Mineral dust, with an emission rate of 1000–3000 Tg per year, is the second most important type of aerosol particle.<sup>1–3</sup> Originating from windblown soil, mineral dusts have similar chemical components to crustal rock, in which aluminum, iron, calcium, and magnesium oxides are the abundant dominant oxides.<sup>4,5</sup> The rich defects, oxygen species, hydroxyls and metal atoms on those oxides provide many reactive sites for the adsorption and transformation of atmospheric trace gases, participating in the formation of new particles and aging existing aerosols.<sup>6–9</sup> Therefore, the reactions of trace gases on mineral dusts, i.e., heterogeneous reactions, are important processes in determining the composition of the gaseous troposphere.<sup>10–12</sup>

Nitrogen dioxide (NO<sub>2</sub>) is one of the most important gaseous pollutants in the atmosphere. The high chemical reactivity of NO<sub>2</sub> makes it an important processor for the formation of acid rain and the depletion of ozone.<sup>13,14</sup> Nitrate coating onto mineral components in aerosols has always been observed in field measurements, suggesting a non-negligible role of heterogeneous atmospheric chemistry in the contribu-

tion of nitrate.<sup>15,16</sup> Laboratory and model studies have confirmed that the heterogeneous reaction of NO<sub>2</sub> on mineral oxides indeed results in the production of nitrate species, which can become an NO<sub>2</sub> sink.<sup>17,18</sup> Moreover, the existence of a mixture of gases causes the heterogeneous formation of significant secondary species on the mineral dusts.<sup>19,20</sup> For example, many studies have focused on the coexisting reactions of SO<sub>2</sub> and NO<sub>2</sub> on mineral dusts, in which a synergistic effect existing in those two gases could remarkably promote the buildup of SO<sub>4</sub><sup>2-</sup> and NO<sub>3</sub><sup>-</sup>, especially during heavy haze periods.<sup>21–23</sup>

Since preindustrial times, NH<sub>3</sub> as an important basic gas, has been injected into the atmosphere at an increasing rate of 2–5-fold that of preindustrial times, with further increases expected over the next 100 years due to the need in agricultural growth.<sup>24</sup> Field observations have established a good correlation between NH<sub>3</sub> and SO<sub>4</sub><sup>2-</sup> and between NO<sub>3</sub><sup>-</sup> and

Received: May 29, 2018

Revised: July 3, 2018

Published: July 11, 2018



$\text{NH}_4^+$  in  $\text{PM}_{2.5}$ .<sup>25</sup> The  $\text{NH}_3$  is considered to be involved in the ternary nucleation process in the  $\text{NH}_3\text{--SO}_2\text{--H}_2\text{O}$  system.<sup>26–29</sup> Notably, environmental chamber modeling found that the existing surface of the aerosol played a positive role in the degradation of precursor gases (i.e.,  $\text{SO}_2$ ,  $\text{NO}_2$ , and  $\text{NH}_3$ ) and that the degradation rates of these precursor gases increased with an increase in the initial ratio of  $(\text{NH}_3)/(\text{NO}_2 + \text{SO}_2)$ .<sup>30</sup> Our recent lab study found that the existence of  $\text{NH}_3$  led to the synergistic formation of  $\text{SO}_4^{2-}$  and  $\text{NH}_4^+$  on typical mineral dusts.<sup>31</sup> Obviously, the  $\text{NH}_3$  plays an important role in the heterogeneous atmospheric chemistry. While its role in the formation of nitrate or its role relative to  $\text{NO}_2$  in the formation of sulfate on mineral dusts in the multigas coexisting system is still paid little attention in lab study.

Actually, the heterogeneous reactivity depends greatly on the properties of mineral oxides, such as the acid–base nature, or the redox properties.<sup>31–34</sup> For the heterogeneous reaction of  $\text{NO}_2$ , basic  $\text{MgO}$  and  $\text{CaO}$  were more active than acidic  $\text{SiO}_2$ .<sup>35</sup> A similar phenomenon also occurred with the heterogeneous reaction of  $\text{SO}_2$  in which, among the same category group as  $\text{Al}_2\text{O}_3$ , the basic  $\text{Al}_2\text{O}_3$  was the most active.<sup>32</sup> Furthermore, as a ubiquitous oxide in soil as well as in rust coatings and bricks,  $\text{Fe}_2\text{O}_3$ , with its unique  $\text{Fe}^{2+}/\text{Fe}^{3+}$  redox chemistry, favors the formation of  $\text{SO}_4^{2-}$  and the heterogeneous conversion of  $\text{NO}_2$ .<sup>32,33,36–38</sup> However, few studies have focused on the relationship of the oxide nature (including acid–base and redox properties) with its heterogeneous reactivity in multigas coexisting system.

In the present study,  $\alpha\text{-Fe}_2\text{O}_3$ ,  $\alpha\text{-Al}_2\text{O}_3$ , and  $\text{CaO}$  and  $\text{MgO}$  particles were chosen as model mineral oxides to investigate the effect of  $\text{NH}_3$  on the heterogeneous reaction of  $\text{NO}_2$  as well as on the complex coexisting system of  $\text{SO}_2$ ,  $\text{NO}_2$  and  $\text{NH}_3$ . The surface products were detected in detail and quantitatively via *in situ* diffuse reflectance infrared Fourier transform spectroscopy (DRIFTS) combined with ion chromatography (IC) techniques. Possible mechanisms and atmospheric implications were further proposed.

## 2. MATERIALS AND METHODS

**2.1. Materials.**  $\alpha\text{-Fe}_2\text{O}_3$  was prepared using a precipitation method, as we previously reported, while  $\alpha\text{-Al}_2\text{O}_3$  was obtained after the calcination of  $\text{AlOOH}$  (SASOL) at 1200 °C.<sup>31</sup>  $\text{CaO}$  and  $\text{MgO}$  were purchased from Sinopharm Chemical Reagent Beijing Co., Ltd. The Brunauer–Emmett–Teller (BET) surface areas of  $\alpha\text{-Fe}_2\text{O}_3$ ,  $\alpha\text{-Al}_2\text{O}_3$ ,  $\text{CaO}$ , and  $\text{MgO}$  were 24.5, 5.5, 57.8, and 29.1  $\text{m}^2 \text{g}^{-1}$ , respectively, as measured by a Quantachrome Quadrasorb SI-MP. X-ray diffraction (XRD) patterns of those samples were confirmed on a computerized PANalytical X'Pert Pro diffractometer equipped with a  $\text{Cu K}\alpha$  radiation source (Figure S1).  $\text{SO}_2$  standard gas (25 ppm in  $\text{N}_2$ , Beijing Huayuan Gases Inc.),  $\text{NO}_2$  standard gas (25 ppm in  $\text{N}_2$ , Beijing Huayuan Gases Inc.),  $\text{NH}_3$  standard gas (36 ppm in  $\text{N}_2$ , Beijing Huayuan Gases Inc.), and high-purity  $\text{N}_2$  and  $\text{O}_2$  (99.999%, Beijing AP BEIFEN Gases Inc.) were used as the gas mixture.

**2.2. *In situ* DRIFTS Experiments.** The *in situ* DRIFTS experiments were performed on an FTIR spectrometer (Nicolet iS50, ThermoFisher Scientific Co., USA) equipped with a high-sensitivity MCT/A detector cooled by liquid nitrogen. Before each experiment, the sample was pretreated at 573 K for 120 min in a stream of synthetic air (80%  $\text{N}_2$  and 20%  $\text{O}_2$ ) of 100  $\text{mL min}^{-1}$  to remove adsorbed species. The sample was then cooled down at 303 K until the baseline

became stable and subsequently exposed to 1 ppmv  $\text{NO}_2$ , 1 ppmv  $\text{SO}_2$ , or/and 1 ppmv  $\text{NH}_3$  for 8–9 h. All the spectra were recorded at a resolution of 4  $\text{cm}^{-1}$  for 30 scans in the spectral range of 4000 to 600  $\text{cm}^{-1}$ .

**2.3. IC Measurements.** IC was used to measure the surface products formed on the samples. The reacted particles were preserved with 1% formaldehyde, which was diluted with ultrapure water (after boiling for 20 min to remove dissolved oxygen) to 10 mL (specific resistance  $\geq 18.2 \text{ M}\Omega \text{ cm}$ ) and then sonicated for 30 min at 298 K. The leaching solution was obtained through a 0.22  $\mu\text{m}$  PTFE membrane filter and then was analyzed using Wayee IC-6200 ion chromatography equipped with TSKgel Super IC-CR cationic or SI-524E anionic analytical column. An eluent of 3.5 mM  $\text{Na}_2\text{CO}_3$  was used at a flow rate of 0.8  $\text{mL min}^{-1}$ . The nitrate and sulfate ions separated by anionic column appeared at 5.344 and 7.532 min successively, while the ammonium ions separated by cationic column was detected at 7.843 min (Figure S2).

## 3. RESULTS

**3.1. Role of  $\text{NH}_3$  in the  $\text{NO}_2\text{--NH}_3\text{--Mineral Dust System.}$**  To investigate the effect of  $\text{NH}_3$  on the heterogeneous reactions of  $\text{NO}_2$  on mineral dusts, *in situ* DRIFTS experiments were performed in a gas flow mixture of 1 ppmv  $\text{NO}_2$  and 1 ppmv  $\text{NH}_3$  balanced with synthetic air at room temperature (303 K). The DRIFTS spectra are shown in Figure 1. The absorption bands and their detailed assignments

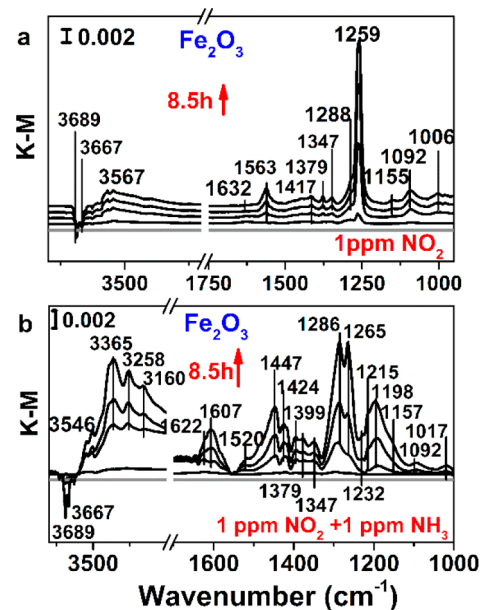


**Figure 1.** (a) *In situ* DRIFTS spectra of individual reaction of 1 ppmv  $\text{NO}_2$  and (b) simultaneous reaction of 1 ppmv  $\text{NO}_2$  and 1 ppmv  $\text{NH}_3$  on  $\alpha\text{-Fe}_2\text{O}_3$  as a function of time.

are given in Table 1. Figure 1a shows the DRIFTS spectra of an individual reaction of  $\text{NO}_2$  over  $\alpha\text{-Fe}_2\text{O}_3$  as a function of time. Several bands ranging over 1600–1000  $\text{cm}^{-1}$  appeared and grew in intensity as time increased. The bands between 1600 and 1200  $\text{cm}^{-1}$  are assigned to the degenerate  $\nu_3$  mode of nitrate species coordinated onto the surface.<sup>39</sup> Generally,  $\nu_3$  can split into two bands, one at a higher wavenumber ( $\nu_{3,\text{high}}$ ) and one at a lower wavenumber ( $\nu_{3,\text{low}}$ ), varying due to the different bonding configurations of monodentate, bidentate



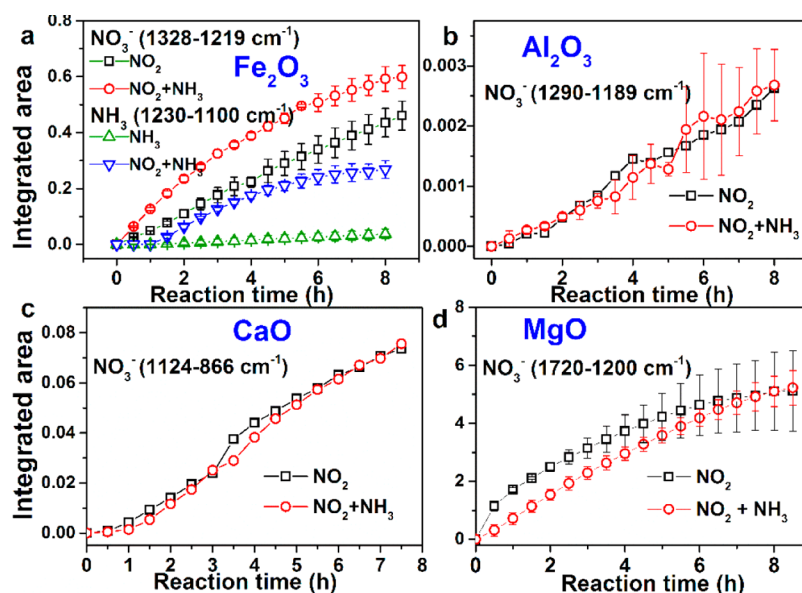


**Figure 3.** Comparison of the integrated areas obtained from DRIFTS spectra over (a)  $\alpha\text{-Fe}_2\text{O}_3$  ( $\text{NO}_3^-$ , 1328–1219  $\text{cm}^{-1}$ ;  $\text{NH}_4^+$ , 1230–1100  $\text{cm}^{-1}$ ), (b)  $\alpha\text{-Al}_2\text{O}_3$  ( $\text{NO}_3^-$ , 1290–1189  $\text{cm}^{-1}$ ), (c) CaO ( $\text{NO}_3^-$ , 1124–866  $\text{cm}^{-1}$ ), and (d) MgO ( $\text{NO}_3^-$ , 1720–1200  $\text{cm}^{-1}$ ) under individual and simultaneous conditions. The error bar represents the standard deviation from three repeated experiments.

To clearly illustrate the interaction between  $\text{NO}_2$  and  $\text{NH}_3$  on dust particles, the final DRIFTS spectra for the individual and simultaneous reactions are compared in Figure 2. On  $\alpha\text{-Fe}_2\text{O}_3$  (Figure 2a),  $\text{NH}_3$  adsorbed predominantly on the Lewis acid sites (3365, 3268, 1604, and 1185  $\text{cm}^{-1}$ ) after the individual reaction for 8.5 h. When  $\text{NO}_2$  and  $\text{NH}_3$  coexisted in the gas flow for 8.5 h, the  $\text{NH}_3$  absorption band at 1185  $\text{cm}^{-1}$  grew in intensity and blue-shifted to 1198  $\text{cm}^{-1}$  and the bands at 3365, 3258, and 3160  $\text{cm}^{-1}$  simultaneously increased, indicating the accumulation of  $\text{NH}_3$  adsorbed species.<sup>53</sup> The strengthened adsorption band at 1447  $\text{cm}^{-1}$  indicated that an increasing amount of  $\text{NH}_3$  preferentially converted into  $\text{NH}_4^+$  with the coexistence of  $\text{NO}_2$ . With respect to the  $\text{NO}_2$ , the addition of  $\text{NH}_3$  not only promoted the accumulation of nitrate, as mentioned above but also led to the increase of nitro–nitrito species at the bands of 1215 and 1157  $\text{cm}^{-1}$ .<sup>19,38</sup>

$\alpha\text{-Al}_2\text{O}_3$ , CaO, and MgO as typical acidic and basic oxides were used further to investigate the influence of  $\text{NH}_3$  on the heterogeneous reaction of  $\text{NO}_2$  (Figure 2b–d). Their detailed reactions with  $\text{NO}_2$  in the absence and presence of  $\text{NH}_3$  versus time are provided in Figure S3. In the individual reaction (Figure 2b),  $\text{NO}_2$  interacted weakly with  $\alpha\text{-Al}_2\text{O}_3$ , with the formation of a relatively small amount of bidentate nitrates at the bands of 1590 ( $\nu_{3,\text{high}}$ ) and 1265  $\text{cm}^{-1}$  ( $\nu_{3,\text{low}}$ ).<sup>29,43</sup> The absorption configurations of nitrate on  $\alpha\text{-Al}_2\text{O}_3$  showed some similarity with that on  $\alpha\text{-Fe}_2\text{O}_3$ , although the latter exhibited a much higher activity toward the adsorption of  $\text{NO}_2$ . By comparison, the adsorption of  $\text{NO}_2$  was favorable on basic CaO and MgO with bridging nitrates (at the bands of 1623, 972, 807  $\text{cm}^{-1}$  on CaO, and 1654  $\text{cm}^{-1}$  on MgO) prevailing on the surfaces.<sup>40,41,47,48</sup> In addition to solvated nitrate (1333 and 848  $\text{cm}^{-1}$  on CaO, and 1364  $\text{cm}^{-1}$  on MgO), some bidentate nitrate (at bands of 1596, 1266, 1061  $\text{cm}^{-1}$  on CaO) and monodentate nitrate (at band of 1522  $\text{cm}^{-1}$  on MgO) were also found over those two types of basic oxides. In the case of  $\text{NH}_3$ , almost no adsorption was observed on CaO and MgO and only weak adsorption of  $\text{NH}_3$  (3356, 3285, 1617, and 1230  $\text{cm}^{-1}$ ) on Lewis acid sites was present on  $\alpha\text{-Al}_2\text{O}_3$ .

After exposure to both  $\text{NO}_2$  and  $\text{NH}_3$  for 8.5 h, no positive influence of  $\text{NH}_3$  on the formation of nitrate was observed for  $\alpha\text{-Al}_2\text{O}_3$ , CaO, and MgO. For  $\alpha\text{-Al}_2\text{O}_3$ , it was possibly due to its extremely low surface area while for CaO and MgO, the surface basicity may not be in favor of the adsorption of  $\text{NH}_3$  and further the interaction of  $\text{NH}_3$  with  $\text{NO}_2$ . Noting the enhanced disturbance in the OH region ranging from 3731 to 3605  $\text{cm}^{-1}$  in the simultaneous reaction on CaO, an intense interaction of OH with the reactants occurred due to the coexistence of  $\text{NO}_2$  and  $\text{NH}_3$ .

To better clarify the effect of  $\text{NH}_3$  on the heterogeneous reactions of  $\text{NO}_2$  on mineral dusts, the integrated areas obtained under different conditions versus the reaction time are exhibited in Figure 3. As seen from Figure 3a, a significant synergistic effect between  $\text{NO}_2$  and  $\text{NH}_3$  was observed on the surface of  $\alpha\text{-Fe}_2\text{O}_3$ . Because of the poorly observed bands for the adsorbed  $\text{NH}_3$  on  $\alpha\text{-Al}_2\text{O}_3$ , only the integrated area for the  $\text{NO}_3^-$  bands is given here (Figure 3b). Almost no obvious promotion effect of  $\text{NH}_3$  was detected during its interaction with  $\text{NO}_2$ . Similar results were also found over CaO and MgO (Figure 3c,d). These proved that the promotion effect of  $\text{NH}_3$  for the heterogeneous reaction of  $\text{NO}_2$  was more obvious on acidic oxides than on basic oxides.

**3.2. Role of  $\text{NH}_3$  in the  $\text{NO}_2\text{--SO}_2\text{--NH}_3\text{--Mineral Dust Coexisting System.}$**  The above-mentioned results suggested a promotion effect of  $\text{NH}_3$  for the formation of nitrate species on mineral dusts. Our recent research has also indicated that the presence of  $\text{NH}_3$  could promote the heterogeneous formation of sulfate/sulfite species. The acid–base interaction was proposed to be responsible for the synergistic effect between  $\text{SO}_2$  and  $\text{NH}_3$  on the surface of mineral dust.<sup>31</sup> As reported previously, the coexistence of  $\text{NO}_2$  with  $\text{SO}_2$  promotes the formation of sulfate significantly through a redox process, in which the dimer intermediate,  $\text{N}_2\text{O}_4$ , of the adsorbed  $\text{NO}_2$  oxidized the adsorbed  $\text{SO}_2$  to form a sulfate species, while  $\text{N}_2\text{O}_4$  was reduced to form a nitrite species,<sup>8,54</sup> as shown below,



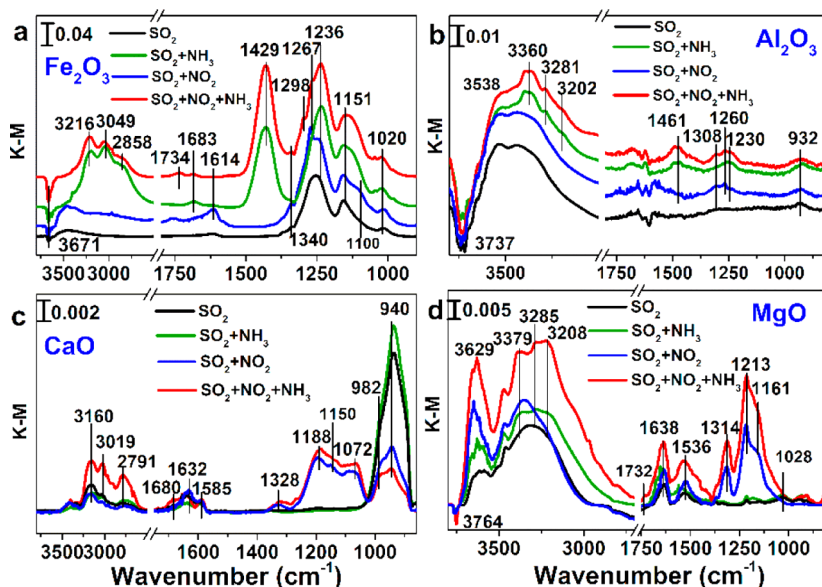


**Figure 4.** Comparison of the final DRIFTS spectra for (a)  $\alpha$ -Fe<sub>2</sub>O<sub>3</sub>, (b)  $\alpha$ -Al<sub>2</sub>O<sub>3</sub>, (c) CaO, and (d) MgO after the reaction with different gas components for 8.5 h.



Given the complex evolution relationship among those gases, it is necessary to elucidate the effect of NH<sub>3</sub> in the mixed SO<sub>2</sub>–NO<sub>2</sub>–NH<sub>3</sub> atmospheres. Therefore, SO<sub>2</sub> was further added into the reaction system, and the heterogeneous formation of SO<sub>4</sub><sup>2-</sup>, NH<sub>4</sub><sup>+</sup>, and NO<sub>3</sub><sup>-</sup> versus time is exhibited in detail in Figures S4 and S5. The final DRIFTS curves for the mineral oxides after exposure to different atmospheres for 8.5 h are thereafter compared in Figure 4.

Compared to the individual reaction of SO<sub>2</sub>, the formation of sulfate was clearly promoted in the presence of NH<sub>3</sub> on acidic Fe<sub>2</sub>O<sub>3</sub>, which was indicated by the growth of the bands at 1236, 1151, and 1020 cm<sup>-1</sup> (Figure 4a, green line).<sup>37</sup> In contrast, this promotion effect was weakly observed on Al<sub>2</sub>O<sub>3</sub>, CaO, and MgO, especially for the latter two basic oxides (Figure 4b–d, green lines). Only sulfite species were detected on Al<sub>2</sub>O<sub>3</sub> and CaO, and the corresponding bands were present at 932 and 940 cm<sup>-1</sup>, respectively. The adsorption of SO<sub>2</sub> on MgO with the coexistence of NH<sub>3</sub> was similar to that without NH<sub>3</sub> and that the weak formation of sulfate and sulfite appeared separately at the bands of 1213 and 1028 cm<sup>-1</sup>.<sup>8</sup> In the SO<sub>2</sub> and NH<sub>3</sub> reaction group, the adsorption of NH<sub>4</sub><sup>+</sup> bound to the Brønsted acid sites was predominant on Fe<sub>2</sub>O<sub>3</sub>, which was represented with the bands of 1683 and 1429 cm<sup>-1</sup> attributed to  $\delta_s(\text{NH}_4^+)$  and  $\delta_{as}(\text{NH}_4^+)$ , which were connected to  $\nu(\text{NH}_4^+)$  in the high-frequency region, at 3049 and 2858 cm<sup>-1</sup>. In addition, a single adsorption band for  $\nu(\text{NH}_3)$  on the Lewis acid site was still observed at 3216 cm<sup>-1</sup>.<sup>31</sup> For Al<sub>2</sub>O<sub>3</sub>, the formation of NH<sub>4</sub><sup>+</sup> on Brønsted acid sites at the band of 1461 cm<sup>-1</sup> ( $\delta_{as}(\text{NH}_4^+)$ ) and the adsorption of NH<sub>3</sub> on Lewis acid sites at the bands of 3360, 3281, 3202 cm<sup>-1</sup> ( $\nu(\text{NH}_3)$ ) and 1230 cm<sup>-1</sup> ( $\delta_s(\text{NH}_3)$ ) were both present.<sup>31</sup> However, the bands assigned to adsorbed NH<sub>3</sub> were far weaker than the broad adsorption of H<sub>2</sub>O at the band of 3538 cm<sup>-1</sup>. The adsorption of NH<sub>3</sub> on CaO and MgO was barely observed possibly due to their basic nature.

The SO<sub>2</sub> reaction in the presence of NO<sub>2</sub> was different (Figure 4, blue lines). In contrast to the experiments with SO<sub>2</sub> and SO<sub>2</sub> + NH<sub>3</sub>, additional sulfate bands at 1340 and 1100

cm<sup>-1</sup> appeared on the surface of Fe<sub>2</sub>O<sub>3</sub> and at 1308 cm<sup>-1</sup> on Al<sub>2</sub>O<sub>3</sub>.<sup>55,56</sup> More obviously, the intensities of the bands at 1188, 1150, and 1072 cm<sup>-1</sup>, which corresponded to the newly formed sulfate species, were very strong on CaO, accompanied by the significant reduction of sulfite species at the band of 940 cm<sup>-1</sup>.<sup>48</sup> For MgO, a large amount of sulfate accumulated on the surface, which was characteristic of the remarkably increasing bands at 1213 and 1161 cm<sup>-1</sup>. In addition, the weak adsorption of sulfite species at the band of 1028 cm<sup>-1</sup> vanished at the same time.<sup>57</sup>

With regard to the NO<sub>2</sub>-adsorbed species, the bands at 1328 cm<sup>-1</sup> for CaO and 1314 cm<sup>-1</sup> for MgO were due to solvated nitrate and ion-coordinated nitrate, respectively.<sup>41</sup> Some nitrate bands, such as 1267 cm<sup>-1</sup> on Fe<sub>2</sub>O<sub>3</sub>, 1260 cm<sup>-1</sup> on Al<sub>2</sub>O<sub>3</sub>, and 982 cm<sup>-1</sup> on CaO, partially overlapped with those assigned to sulfate species, while others mostly appeared at the bands ranging from 1683 to 1536 cm<sup>-1</sup>. The weak adsorption of N<sub>2</sub>O<sub>4</sub> was also observed at approximately 1732 cm<sup>-1</sup> on Fe<sub>2</sub>O<sub>3</sub> and MgO.<sup>8,19</sup> These results confirmed that NO<sub>2</sub> promoted the oxidation of SO<sub>2</sub> to sulfate, which largely proceeded through the above-mentioned redox process (eq 1). While the promotion effect by NH<sub>3</sub> can be driven by the acid–base interaction since no transformation from sulfite to sulfate occurred in this situation. Essentially, those results align with our previous findings.<sup>8,31</sup>

When SO<sub>2</sub>, NH<sub>3</sub>, and NO<sub>2</sub> coexisted in the gas flow (Figure 4, red lines), the NH<sub>3</sub> adsorption was obviously enhanced in the high-wavenumber region from 3400 to 2800 cm<sup>-1</sup>, particularly for the basic oxides of CaO and MgO. Meanwhile, the growth of the sulfate bands (1188 and 1072 cm<sup>-1</sup>) on CaO, and the increase of both the sulfate (1314, 1213, and 1161 cm<sup>-1</sup>) and nitrate (1638 and 1536 cm<sup>-1</sup>) bands on MgO were also observed. By comparison, the synchronous growth of SO<sub>4</sub><sup>2-</sup>, NO<sub>3</sub><sup>-</sup>, and NH<sub>4</sub><sup>+</sup> was not evident on Fe<sub>2</sub>O<sub>3</sub> and Al<sub>2</sub>O<sub>3</sub>. A slight increase in the NH<sub>4</sub><sup>+</sup> at band of 1429 cm<sup>-1</sup> and the formation of a new sulfate band at 1298 cm<sup>-1</sup> occurred on the former, while only a weak enhancement of the NH<sub>4</sub><sup>+</sup> band at 1461 cm<sup>-1</sup> was shown on the latter. On the basis of the DRIFTS results, the acid–base interaction between NO<sub>2</sub>/SO<sub>2</sub>

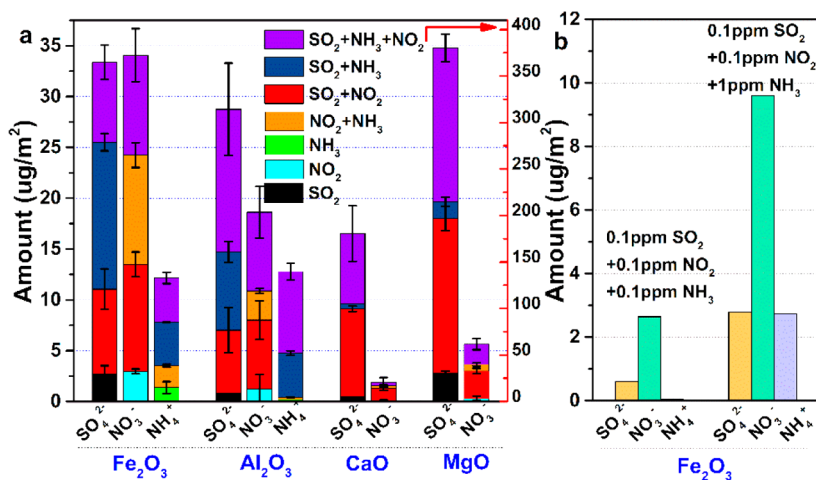


**Figure 5.** IC results showing the quantity of surface products formed on the reacted particles, which were collected from the DRIFTS cell after reactions under different conditions for 8.5 h. All the concentrations of reactants in (a) were 1 ppmv, and the amounts of  $\text{SO}_4^{2-}$  and  $\text{NO}_3^-$  formed on  $\text{MgO}$  follow the right y-axis, while others follow the left y-axis. The concentration of  $\text{NH}_3$  varied from 0.1 to 1 ppmv in (b), while  $\text{NO}_2$  and  $\text{SO}_2$  remained at a constant concentration of 0.1 ppmv in this case.

with  $\text{NH}_3$  and the redox process between  $\text{NO}_2$  and  $\text{SO}_2$  can both occur with the reactions of the three gases. However, of the two mechanisms, the one that is prioritized might be determined by the properties of mineral oxides.

**3.3. Quantitative Analysis of Surface Products.** To elucidate the role of  $\text{NH}_3$  in the heterogeneous reactions of  $\text{SO}_2$ ,  $\text{NO}_2$ , and  $\text{NH}_3$  on mineral oxides, quantitative analysis of the surface products resulting from those reacted particles in DRIFTS experiments were conducted by IC measurements, as shown in Figure 5. Detailed data that are displayed in Figure 5 have also been summarized in Tables S1 and S2. In Figure 5a, compared to the individual reactions ( $\text{SO}_2/\text{NO}_2/\text{NH}_3$  reaction), two kinds of gases ( $\text{SO}_2$  and  $\text{NH}_3$ ,  $\text{NO}_2$  and  $\text{NH}_3$ ,  $\text{SO}_2$  and  $\text{NO}_2$ ) coexisting in the system resulted in the synergistic formation of  $\text{SO}_4^{2-}$ ,  $\text{NO}_3^-$ , and  $\text{NH}_4^+$  on the mineral oxides. With the coexistence of  $\text{NH}_3$  ( $\text{SO}_2 + \text{NH}_3$ ,  $\text{NO}_2 + \text{NH}_3$ ), its promotion function for the formation of  $\text{SO}_4^{2-}$  and  $\text{NO}_3^-$  was more obvious on acidic  $\text{Fe}_2\text{O}_3$  and  $\text{Al}_2\text{O}_3$  (especially on  $\text{Fe}_2\text{O}_3$ ) than on basic  $\text{CaO}$  and  $\text{MgO}$ . In contrast, the  $\text{NO}_2$  promotion effect played a more predominant role in the formation of  $\text{SO}_4^{2-}$  and  $\text{NO}_3^-$  on the basic oxides of  $\text{CaO}$  and  $\text{MgO}$  in the  $\text{SO}_2 + \text{NO}_2$  reaction group.

However, when the three kinds of gases were introduced into the system simultaneously, the amount of  $\text{SO}_4^{2-}$ ,  $\text{NO}_3^-$ , and  $\text{NH}_4^+$  formed did not further increase, and instead, decreased in comparison with that for the coexistence of  $\text{SO}_2$  and  $\text{NH}_3$  or of  $\text{NO}_2$  and  $\text{NH}_3$  on  $\text{Fe}_2\text{O}_3$  and that for the coexistence of  $\text{SO}_2$  and  $\text{NO}_2$  on  $\text{CaO}$  and  $\text{MgO}$ , but not for  $\text{Al}_2\text{O}_3$ . These results indicate that the acid–base interaction (between  $\text{SO}_2$  and  $\text{NH}_3$  or between  $\text{NO}_2$  and  $\text{NH}_3$ ) and the redox process (between  $\text{SO}_2$  and  $\text{NO}_2$ ) may exhibit a competition effect toward the formation of  $\text{SO}_4^{2-}$ ,  $\text{NO}_3^-$ , and  $\text{NH}_4^+$ .

Taking the evolution of  $\text{SO}_4^{2-}$  on  $\text{Fe}_2\text{O}_3$  as an example, both  $\text{NH}_3$  and  $\text{NO}_2$  would compete for the  $\text{SO}_2$  molecules to induce the transformation of  $\text{SO}_2$  to  $\text{SO}_4^{2-}$ . It seemed that  $\text{NH}_3$  has a more promotional effect than  $\text{NO}_2$  on the formation of  $\text{SO}_4^{2-}$  on this type of acidic oxide. However, with equal inlet concentrations of the reactants,  $\text{NH}_3$  would be limited in the interaction with  $\text{SO}_2$  due to the competition effect of  $\text{NO}_2$ , in that a portion of  $\text{NH}_3$  can also interact with  $\text{NO}_2$ . Therefore,

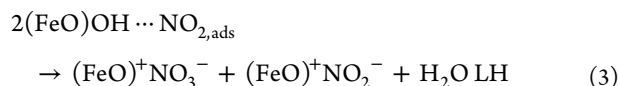
the amount of  $\text{SO}_4^{2-}$  formed under this circumstance would be lower than the amounts formed for the coexisting gases ( $\text{SO}_2$  and  $\text{NH}_3$  or  $\text{SO}_2$  and  $\text{NO}_2$ ). To prove this hypothesis,  $\text{NH}_3$  was increased to up to 10 times the concentration of  $\text{SO}_2$  and  $\text{NO}_2$ , as shown in Figure 5b. All the amounts of  $\text{SO}_4^{2-}$ ,  $\text{NO}_3^-$ , and  $\text{NH}_4^+$  increased significantly compared to those in the low-concentration situation. These results confirmed that both  $\text{SO}_2$  and  $\text{NO}_2$  were favorable for the reaction with  $\text{NH}_3$  on acidic  $\text{Fe}_2\text{O}_3$ ; further investigation is needed to determine which is more attractive to  $\text{NH}_3$  or whether there exists an interaction between  $\text{SO}_2$  and  $\text{NO}_2$ .

For other types of basic oxides of  $\text{CaO}$  and  $\text{MgO}$ , the interaction between  $\text{SO}_2$  and  $\text{NO}_2$  is dominant but can be weakened by the presence of  $\text{NH}_3$ , which may interact with both  $\text{SO}_2$  and  $\text{NO}_2$  at the same time. The case of the weakened promotion effect in the three kinds of gas coexisting system did not occur on  $\text{Al}_2\text{O}_3$ . The results implied that the different roles of  $\text{NH}_3$  (via an acid–base interaction with  $\text{SO}_2$  or  $\text{NO}_2$ ) and  $\text{NO}_2$  (via a redox process with  $\text{SO}_2$ ) are closely related to the properties of the mineral oxides, which will be discussed in detail in a later part.

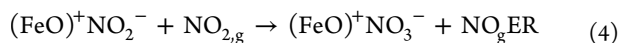
## 4. DISCUSSION

### 4.1. $\text{NO}_2$ – $\text{NH}_3$ –Mineral Dust Reaction System.

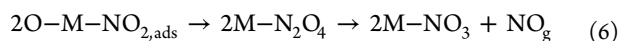
DRIFTS and the IC investigation suggested that the synergistic effect between  $\text{NO}_2$  and  $\text{NH}_3$  and that between  $\text{SO}_2$  and  $\text{NH}_3$  or  $\text{SO}_2$  and  $\text{NO}_2$  vary on mineral oxides with different acidic/basic properties. In the  $\text{NO}_2$  and  $\text{NH}_3$  reaction group, the synergistic formation of  $\text{NO}_3^-$  and  $\text{NH}_4^+$  was clearly detected on acidic  $\text{Fe}_2\text{O}_3$  and  $\text{Al}_2\text{O}_3$ , especially on  $\text{Fe}_2\text{O}_3$ , by both DRIFTS and the IC measurements. The DRIFTS spectra (Figures 1 and 2b) show that the OH groups were the main active sites for the adsorption of  $\text{NO}_2$  on  $\text{Fe}_2\text{O}_3$  and  $\text{Al}_2\text{O}_3$ , which caused the predominant formation of bidentate nitrate on these two types of oxides. This type of nitrate configuration was due to the adsorption of  $\text{NO}_2$  on the hydroxyls, followed by a disproportionation reaction of two adsorbed- $\text{NO}_2$  molecules through the Langmuir–Hinshelwood (LH) mechanism, with  $\alpha\text{-Fe}_2\text{O}_3$  as an example,<sup>18,44</sup>



In this reaction, the production of nitrate was accompanied by the formation of nitrite species, which were confirmed by the presence of bands at ca. 1215, 1157, and 1092  $\text{cm}^{-1}$  on  $\alpha$ - $\text{Fe}_2\text{O}_3$ . Then, the nitrite species were transformed into nitrate rapidly by excess gaseous  $\text{NO}_2$  through the Eley–Rideal (ER) mechanism, as expressed in eq 4,



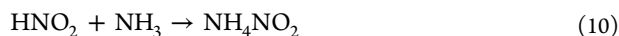
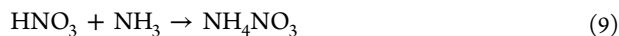
No nitrite and adsorbed NO species were observed on  $\alpha$ - $\text{Al}_2\text{O}_3$ , possibly due to their extreme low concentrations or poor signals. Since the CaO and MgO surfaces were not as hydroxylated as the  $\text{Fe}_2\text{O}_3$  and  $\text{Al}_2\text{O}_3$  surfaces (Figure 2c,d), no consumption of OH groups was observed when  $\text{NO}_2$  reacted individually, and the main product was a bridging nitrate. In this case,  $\text{NO}_2$  may coordinate directly onto the exposed metal atoms (Lewis acid sites), interacting with adjacent adsorbed  $\text{NO}_2$  (possibly in the form of  $\text{N}_2\text{O}_4$ ) to form nitrate and gaseous  $\text{NO}$ .<sup>42</sup> The reaction equations were listed as follows:



In addition, the presence of water on the oxide surface would involve the formation of solvated nitrate (e.g., ca. 1680  $\text{cm}^{-1}$ ) and solvated nitrite species, as shown in eqs 7 and 8:<sup>18,41</sup>



When  $\text{NH}_3$  was introduced simultaneously with the reaction of  $\text{NO}_2$ , it preferentially adsorbed on Lewis acid sites (Figure 1b). The preferential adsorption of  $\text{NH}_3$  (as seen in Figure 1b) quickly increases the surface basicity, promoting the adsorption of  $\text{NO}_2$ . Due to their different adsorption sites,  $\text{NO}_2$  mainly adsorbed on the OH sites while  $\text{NH}_3$  coordinated on the exposed metal atoms, and a synergistic effect can be found on  $\text{Fe}_2\text{O}_3$ .<sup>58</sup> In addition, a small amount of  $\text{NH}_4^+$  (1447  $\text{cm}^{-1}$ ) present on the surface of  $\text{Fe}_2\text{O}_3$  suggests that the nitric or nitrous acid formed through eqs 7 and 8 participated in the neutralization of adsorbed  $\text{NH}_3$ :



Since surface hydroxyls served as the main adsorption sites for water molecules, highly hydroxylated  $\text{Fe}_2\text{O}_3$  was favored for the formation of nitric or nitrous acid through reactions 7 and 8 followed by the formation of  $\text{NH}_4^+$  through reactions 9 and 10.<sup>59–61</sup>

In contrast, no obvious promotion effect of  $\text{NH}_3$  occurred with the formation of  $\text{NO}_3^-$  for basic CaO and MgO. As postulated above,  $\text{NO}_2$  mainly coordinated onto exposed metal atoms, meaning that it competed with  $\text{NH}_3$  for Lewis acid sites. A previous study found that  $\text{NO}_3^-$  had a closer connection to the metal atoms in basic oxide, such as CaO and MgO, than in acidic oxides, such as  $\alpha$ - $\text{Al}_2\text{O}_3$ ,  $\text{TiO}_2$ , and  $\gamma$ - $\text{Fe}_2\text{O}_3$ .<sup>41</sup> The strong bond between  $\text{NO}_3^-$  and Ca (or Mg) in the present study may further limit the adsorption of  $\text{NH}_3$  on the same Ca (or Mg) atoms. However, nitrate connecting to

metal atoms showed a strong electron affinity, which would increase the Lewis acid strength of the metal ion and may promote the adsorption of  $\text{NH}_3$  to certain extent. Furthermore, a small amount of other types of nitrate species including bidentate, monodentate, and solvated nitrate species present on CaO and MgO suggests that a small fraction of  $\text{NO}_2$  did not compete with  $\text{NH}_3$  for the Lewis acid sites, possibly through the reaction in eqs 3 and 4. Therefore, the coexistence with  $\text{NH}_3$  did not reduce the amount of nitrate but promoted its formation slightly, as found from the IC results. The obvious consumption of OH ranging from 3731 to 3605  $\text{cm}^{-1}$  (Figure 2c) in the simultaneous reaction confirms the enhanced interactions of  $\text{NO}_2$  and  $\text{NH}_3$  with the surface, which may account for the additional formation of nitrate and ammonia species on basic oxides.

#### 4.2. $\text{NO}_2$ – $\text{SO}_2$ – $\text{NH}_3$ –Mineral Dust Reaction System.

Since our previous studies have explained the mechanisms regarding the synergistic effect between  $\text{SO}_2$  and  $\text{NH}_3$  and between  $\text{SO}_2$  and  $\text{NO}_2$  in detail, which have been simply mentioned earlier as the acid–base interaction mechanism and redox mechanism, the complex relationship between the  $\text{NH}_3$  (or  $\text{NO}_2$ ) role and the properties of the mineral dusts would be revealed on the basis of these given mechanisms.<sup>8,31</sup> The IC results showed that the synergistic effect between  $\text{SO}_2$  and  $\text{NH}_3$  or between  $\text{NO}_2$  and  $\text{NH}_3$  prevailed over the synergistic effect between  $\text{SO}_2$  and  $\text{NO}_2$  on  $\text{Fe}_2\text{O}_3$ , especially for  $\text{SO}_2$  for the formation of  $\text{SO}_4^{2-}$ , while the reverse was found over CaO and MgO for the formation of  $\text{SO}_4^{2-}$  and  $\text{NO}_3^-$ .

It has been demonstrated that  $\text{SO}_2$  mainly interacted with basic  $\text{O}^{2-}$  sites at the steps and kinks in CaO and MgO to form sulfite species, and only a small amount of sulfate formation can be determined by the four-coordinated oxide anions on the steps and corners of the MgO particles under dry conditions, even in the presence of  $\text{O}_2$ .<sup>57</sup> In the individual reaction of  $\text{SO}_2$  in this work, the amount of sulfate obtained by the IC measurements on CaO and MgO (and  $\text{Al}_2\text{O}_3$ ) can be partially derived from the aqueous oxidation during the measurement process because the dissolved oxygen cannot be excluded completely and the particles might not be preserved very well with formaldehyde. After this correction, the transformation of  $\text{SO}_2$  and  $\text{NO}_2$  to  $\text{SO}_4^{2-}$  and  $\text{NO}_3^-$  still requires an oxidation process, in which CaO and MgO had no oxidizing ability but only  $\text{NO}_2$  can act as an oxidant (Figures 3 and 4, eqs 1–6). Moreover, given the basic nature, CaO and MgO were more favorable for the adsorption of  $\text{NO}_2$  than  $\text{NH}_3$ . Therefore, the synergistic effect between  $\text{SO}_2$  and  $\text{NO}_2$  has a more promotional effect than that between  $\text{SO}_2$  (or  $\text{NO}_2$ ) and  $\text{NH}_3$  for the formation of  $\text{SO}_4^{2-}$ .

The case of  $\text{Fe}_2\text{O}_3$  is somewhat different as  $\text{Fe}_2\text{O}_3$  itself can transform  $\text{SO}_2$  into sulfate species, driven by the Fe(III)/Fe(II) redox process by a series of free-radical propagation, termination, and product-formation reactions, or by molecular oxygen activation on oxygen vacancy sites.<sup>37,62</sup> The DRIFTS spectra showed that the adsorption of  $\text{NH}_3$  was fast, even with the coexistence of  $\text{NO}_2$  (Figure 1b), possibly due to the acidic nature of  $\text{Fe}_2\text{O}_3$ . The quickly enhanced surface basicity would promote the adsorption of  $\text{SO}_2$  rapidly, which then transformed into  $\text{SO}_4^{2-}$  from the Fe(III)/Fe(II) redox process. Furthermore, due to the acidic nature, the adsorption of  $\text{NO}_2$  as a dimer of  $\text{N}_2\text{O}_4$  may be limited, which is a key intermediate promoter for the oxidation of  $\text{SO}_2$ .<sup>8</sup> Therefore, the promotional effect of  $\text{NH}_3$  seemed more obvious than that of  $\text{NO}_2$  in the formation of  $\text{SO}_4^{2-}$  on acidic  $\text{Fe}_2\text{O}_3$ . For another acidic

oxide of  $\text{Al}_2\text{O}_3$ , the promotion effect of  $\text{NH}_3$  was basically equal to that of  $\text{NO}_2$  for the formation of  $\text{SO}_4^{2-}$ . However, neither  $\text{Al}_2\text{O}_3$  nor  $\text{NH}_3$  has the ability to oxidize  $\text{SO}_2$  to  $\text{SO}_4^{2-}$  in the way  $\text{Fe}_2\text{O}_3$  or  $\text{NO}_2$  does. The remarkably increased amount of  $\text{SO}_4^{2-}$  in the presence of  $\text{NH}_3$  was possibly due to the dramatically enhanced adsorption of water, as indicated by the enhanced  $3538\text{ cm}^{-1}$  band in Figure 4b, which was favorable for the conversion of surface-coordinated sulfite to sulfate species.<sup>57</sup>

It is noted that the formation of nitrate species was promoted significantly by  $\text{SO}_2$  on all mineral oxides. One possible reason can be the reoxidation of the produced nitrite in eq 2.<sup>63,64</sup> Especially with the aid of  $\text{O}_2$ , the  $\text{NO}$  resulting from the eqs 4 and 6 would combine with nitrite species to form nitrate species, as shown below,<sup>54</sup>



IC results (Figure 5a) showed that the addition of a third gas did not further increase the amounts of  $\text{SO}_4^{2-}$ ,  $\text{NO}_3^-$ , and  $\text{NH}_4^+$  on  $\text{Fe}_2\text{O}_3$ ,  $\text{CaO}$ , and  $\text{MgO}$  compared to the amounts in the presence of two gases, which was possibly due to the complex competition effect among those synergistic effects ( $\text{SO}_2$  and  $\text{NH}_3$ ,  $\text{NO}_2$  and  $\text{NH}_3$ , and  $\text{SO}_2$  and  $\text{NO}_2$ ) with equivalent gas concentrations. On  $\text{Al}_2\text{O}_3$ , however, the amounts of  $\text{SO}_4^{2-}$  and  $\text{NH}_4^+$  were higher in the  $\text{SO}_2$ ,  $\text{NO}_2$ , and  $\text{NH}_3$  reaction group than in the two-gas reaction groups, indicating that both the acid–base interaction and redox reaction mechanism exhibit a synergistic influence on the formation of  $\text{SO}_4^{2-}$  and  $\text{NH}_4^+$ . The acidic nature of  $\text{Al}_2\text{O}_3$  induced the adsorption of  $\text{NH}_3$ , promoting the adsorption of  $\text{SO}_2$ , which was oxidized into  $\text{SO}_4^{2-}$  by  $\text{NO}_2$  (in the form of  $\text{N}_2\text{O}_4$ ) at the same time. In turn, the formed  $\text{SO}_4^{2-}$  increased the Brønsted acid sites on the surface and then promoted the formation of  $\text{NH}_4^+$ .<sup>31</sup>

## 5. CONCLUSION AND ATMOSPHERIC IMPLICATIONS

The promotional effect of  $\text{NH}_3$  on the heterogeneous formation of  $\text{NO}_3^-$ ,  $\text{SO}_4^{2-}$ , and  $\text{NH}_4^+$  has been elucidated in detail, which relied greatly on the acid–base and redox properties of mineral oxides. For acid oxides such as  $\alpha\text{-Fe}_2\text{O}_3$  and  $\alpha\text{-Al}_2\text{O}_3$ , the  $\text{NH}_3$  exerts a significant promotion effect on the formation of nitrate species. Moreover, it acted as a counterpart role and was even more important relative to the  $\text{NO}_2$  in promoting the formation of  $\text{SO}_4^{2-}$ . Particularly for  $\alpha\text{-Fe}_2\text{O}_3$ , its redox chemistry significantly facilitated the promotional effect of  $\text{NH}_3$ . Evidence from the remarkably formed  $\text{SO}_4^{2-}$ ,  $\text{NO}_3^-$ , and  $\text{NH}_4^+$  under  $\text{NH}_3$ -rich conditions hinted us that an effective control of the emission of  $\text{NH}_3$  might be a potential strategy to reduce secondary inorganic aerosols in  $\text{NH}_3$ -rich areas.<sup>65</sup> However, the prevailing effect of  $\text{NO}_2$  over  $\text{NH}_3$  for the formation of  $\text{SO}_4^{2-}$  and  $\text{NO}_3^-$  on basic  $\text{CaO}$  and  $\text{MgO}$  is indicative of a more effective way to reduce the formation of secondary species in areas containing an abundance of basic aerosols.<sup>21,66</sup> Given the varied mineralogy of dusts with source location, a differential elaboration of the evolution mechanism of secondary species is necessary.

In the system involving the reaction with the coexistence of  $\text{SO}_2$ ,  $\text{NO}_2$ , and  $\text{NH}_3$  sharing equal inlet concentrations, however, the synergistic effect initiated separately by  $\text{NO}_2$  or  $\text{NH}_3$  will not multiply to obtain further enhanced formation of  $\text{SO}_4^{2-}$ ,  $\text{NO}_3^-$ , and  $\text{NH}_4^+$  on the oxides with redox or basic properties. Nevertheless, the IC results of  $\alpha\text{-Al}_2\text{O}_3$  illustrate that acidic oxides with nonoxidizing ability are favorable

toward the synergistic adsorption of  $\text{SO}_2$  (or  $\text{NO}_2$ ) and  $\text{NH}_3$  (driven by  $\text{NH}_3$ ) and the simultaneously transformation of  $\text{SO}_2$  (or  $\text{NO}_2$ ) and  $\text{NH}_3$  into  $\text{SO}_4^{2-}$  (or  $\text{NO}_3^-$ ) and  $\text{NH}_4^+$  (oxidized by  $\text{NO}_2$ ). Thus, an enhanced synergistic effect is expected on this type of acid oxide in the system of coexisting  $\text{SO}_2$ ,  $\text{NO}_2$  and  $\text{NH}_3$ .

## ■ ASSOCIATED CONTENT

### Supporting Information

The Supporting Information is available free of charge on the ACS Publications website at DOI: 10.1021/acs.jpca.8b05130.

XRD patterns of mineral oxides, chromatogram of  $\text{NO}_3^-$ ,  $\text{SO}_4^{2-}$ , and  $\text{NH}_4^+$ , *in situ* DRIFTS spectra of mineral oxides during exposure to different reaction atmospheres versus reaction time, tables summarizing the amounts of surface products formed on mineral oxides under different conditions (PDF)

## ■ AUTHOR INFORMATION

### Corresponding Author

\*Qingxin Ma. E-mail: qxma@rcees.ac.cn. Tel: 86-10-62849337. Fax: 86-10-62849337.

### ORCID

Weiwei Yang: 0000-0002-9227-0459

Qingxin Ma: 0000-0002-9668-7008

Jinzhu Ma: 0000-0003-1878-0669

### Notes

The authors declare no competing financial interest.

## ■ ACKNOWLEDGMENTS

This research was financially supported by the National Key R&D Program of China (2016YFC0202700), the National Natural Science Foundation of China (91744205), and the Project funded by China Postdoctoral Science Foundation (no. 2017M622485).

## ■ REFERENCES

- (1) Buseck, P. R.; Posfai, M. L. Airborne minerals and related aerosol particles: Effects on climate and the environment. *Proc. Natl. Acad. Sci. U. S. A.* **1999**, *96*, 3372–3379.
- (2) Engelbrecht, J. P.; Derbyshire, E. Airborne Mineral Dust. *Elements* **2010**, *6*, 241–246.
- (3) Ginoux, P.; Prospero, J. M.; Gill, T. E.; Hsu, N. C.; Zhao, M. Global-scale attribution of anthropogenic and natural dust sources and their emission rates based on MODIS Deep Blue aerosol products. *Rev. Geophys.* **2012**, *50*, RG3005.
- (4) Usher, C. R.; Michel, A. E.; Grassian, V. H. Reactions on Mineral Dust. *Chem. Rev.* **2003**, *103*, 4883–4939.
- (5) Tang, M.; Cziczo, D. J.; Grassian, V. H. Interactions of Water with Mineral Dust Aerosol: Water Adsorption, Hygroscopicity, Cloud Condensation, and Ice Nucleation. *Chem. Rev.* **2016**, *116*, 4205–4259.
- (6) Pacchioni, G. Oxygen vacancy: the invisible agent on oxide surfaces. *ChemPhysChem* **2003**, *4*, 1041–1047.
- (7) Al-Abadleh, H. A.; Grassian, V. H. Oxide surfaces as environmental interfaces. *Surf. Sci. Rep.* **2003**, *52*, 63–161.
- (8) Liu, C.; Ma, Q.; Liu, Y.; Ma, J.; He, H. Synergistic reaction between  $\text{SO}_2$  and  $\text{NO}_2$  on mineral oxides: a potential formation pathway of sulfate aerosol. *Phys. Chem. Chem. Phys.* **2012**, *14*, 1668–1676.
- (9) Dentener, F. J.; Carmichael, G. R.; Zhang, Y.; Lelieveld, J.; Crutzen, P. J. Role of mineral aerosol as a reactive surface in the global troposphere. *J. Geophys. Res.* **1996**, *101*, 22869–22889.

- (10) Ravishankara, A. R. Heterogeneous and Multiphase Chemistry in the Troposphere. *Science* **1997**, *276*, 1058–1065.
- (11) Crowley, J. N.; Ammann, M.; Cox, R. A.; Hynes, R. G.; Jenkin, M. E.; Mellouki, A.; Rossi, M. J.; Troe, J.; Wallington, T. J. Evaluated kinetic and photochemical data for atmospheric chemistry: Volume V – heterogeneous reactions on solid substrates. *Atmos. Chem. Phys.* **2010**, *10*, 9059–9223.
- (12) Tang, M.; Huang, X.; Lu, K.; Ge, M.; Li, Y.; Cheng, P.; Zhu, T.; Ding, A.; Zhang, Y.; Gligorovski, S.; Song, W.; Ding, X.; Bi, X.; Wang, X. Heterogeneous reactions of mineral dust aerosol: implications for tropospheric oxidation capacity. *Atmos. Chem. Phys.* **2017**, *17*, 11727–11777.
- (13) Jacob, D. J. Heterogeneous chemistry and tropospheric ozone. *Atmos. Environ.* **2000**, *34*, 2131–2159.
- (14) Brimblecombe, P.; Stedman, D. H. Historical evidence for a dramatic increase in the nitrate component of acid-rain. *Nature* **1982**, *298*, 460–462.
- (15) Li, W. J.; Shao, L. Y. Observation of nitrate coatings on atmospheric mineral dust particles. *Atmos. Chem. Phys.* **2009**, *9*, 1863–1871.
- (16) Sullivan, R. C.; Guazzotti, S. A.; Sodeman, D. A.; Prather, K. A. Direct observations of the atmospheric processing of Asian mineral dust. *Atmos. Chem. Phys.* **2007**, *7*, 1213–1236.
- (17) Goodman, A. L.; Underwood, G. M.; Grassian, V. H. Heterogeneous Reaction of NO<sub>2</sub>: Characterization of Gas-Phase and Adsorbed Products from the Reaction, 2NO<sub>2</sub>(g) + H<sub>2</sub>O(a) - HONO(g) + HNO<sub>3</sub>(a) on Hydrated Silica Particles. *J. Phys. Chem. A* **1999**, *103*, 7217–7223.
- (18) Borensen, C.; Kirchner, U.; Scheer, V.; Vogt, R.; Zellner, R. Mechanism and Kinetics of the Reactions of NO<sub>2</sub> or HNO<sub>3</sub> with Alumina as a Mineral Dust Model Compound. *J. Phys. Chem. A* **2000**, *104*, 5036–5045.
- (19) Niu, H.; Li, K.; Chu, B.; Su, W.; Li, J. Heterogeneous Reactions between Toluene and NO<sub>2</sub> on Mineral Particles under Simulated Atmospheric Conditions. *Environ. Sci. Technol.* **2017**, *51*, 9596–9604.
- (20) Ma, Q.; Wang, T.; Liu, C.; He, H.; Wang, Z.; Wang, W.; Liang, Y. SO<sub>2</sub> Initiates the Efficient Conversion of NO<sub>2</sub> to HONO on MgO Surface. *Environ. Sci. Technol.* **2017**, *51*, 3767–3775.
- (21) He, H.; Wang, Y.; Ma, Q.; Ma, J.; Chu, B.; Ji, D.; Tang, G.; Liu, C.; Zhang, H.; Hao, J. Mineral dust and NO<sub>x</sub> promote the conversion of SO<sub>2</sub> to sulfate in heavy pollution days. *Sci. Rep.* **2015**, *4*, 4172–4176.
- (22) Zheng, B.; Zhang, Q.; Zhang, Y.; He, K. B.; Wang, K.; Zheng, G. J.; Duan, F. K.; Ma, Y. L.; Kimoto, T. Heterogeneous chemistry: a mechanism missing in current models to explain secondary inorganic aerosol formation during the January 2013 haze episode in North China. *Atmos. Chem. Phys.* **2015**, *15*, 2031–2049.
- (23) Wang, G.; Zhang, R.; Gomez, M. E.; Yang, L.; Levy Zamora, M.; Hu, M.; Lin, Y.; Peng, J.; Guo, S.; Meng, J.; Li, J.; Cheng, C.; Hu, T.; Ren, Y.; Wang, Y.; Gao, J.; Cao, J.; An, Z.; Zhou, W.; Li, G.; Wang, J.; Tian, P.; Marrero-Ortiz, W.; Secrest, J.; Du, Z.; Zheng, J.; Shang, D.; Zeng, L.; Shao, M.; Wang, W.; Huang, Y.; Wang, Y.; Zhu, Y.; Li, Y.; Hu, J.; Pan, B.; Cai, L.; Cheng, Y.; Ji, Y.; Zhang, F.; Rosenfeld, D.; Liss, P. S.; Duce, R. A.; Kolb, C. E.; Molina, M. J. Persistent sulfate formation from London Fog to Chinese haze. *Proc. Natl. Acad. Sci. U. S. A.* **2016**, *113*, 13630–13635.
- (24) Reis, S.; Pinder, R. W.; Zhang, M.; Lijie, G.; Sutton, M. A. Reactive nitrogen in atmospheric emission inventories. *Atmos. Chem. Phys.* **2009**, *9*, 7657–7677.
- (25) Behera, S. N.; Sharma, M. Investigating the potential role of ammonia in ion chemistry of fine particulate matter formation for an urban environment. *Sci. Total Environ.* **2010**, *408*, 3569–3575.
- (26) Korhonen, P.; Kulmala, M.; Laaksonen, A.; Viisanen, Y.; McGraw, R.; Seinfeld, J. H. Ternary nucleation of H<sub>2</sub>SO<sub>4</sub>, NH<sub>3</sub>, and H<sub>2</sub>O in the atmosphere. *J. Geophys. Res.* **1999**, *104*, 26349–26353.
- (27) Coffman, D. J.; Hegg, D. A. A Preliminary study of the effect of ammonia on particle nucleation in the marine boundary layer. *J. Geophys. Res.* **1995**, *100*, 7147–7160.
- (28) Kulmala, M.; Pirjola, L.; Mäkelä, J. M. Stable sulphate clusters as a source of new atmospheric particles. *Nature* **2000**, *404*, 66–69.
- (29) Zhang, R.; Khalizov, A.; Wang, L.; Hu, M.; Xu, W. Nucleation and growth of nanoparticles in the atmosphere. *Chem. Rev.* **2012**, *112*, 1957–2011.
- (30) Behera, S. N.; Sharma, M. Degradation of SO<sub>2</sub>, NO<sub>2</sub> and NH<sub>3</sub> leading to formation of secondary inorganic aerosols: An environmental chamber study. *Atmos. Environ.* **2011**, *45*, 4015–4024.
- (31) Yang, W.; He, H.; Ma, Q.; Ma, J.; Liu, Y.; Liu, P.; Mu, Y. Synergistic formation of sulfate and ammonium resulting from reaction between SO<sub>2</sub> and NH<sub>3</sub> on typical mineral dust. *Phys. Chem. Chem. Phys.* **2016**, *18*, 956–964.
- (32) Zhang, X.; Zhuang, G.; Chen, J.; Wang, Y.; Wang, X.; An, Z.; Zhang, P. Heterogeneous reactions of sulfur dioxide on typical mineral particles. *J. Phys. Chem. B* **2006**, *110*, 12588–12596.
- (33) Li, G.; Bei, N.; Cao, J.; Huang, R.; Wu, J.; Feng, T.; Wang, Y.; Liu, S.; Zhang, Q.; Tie, X.; Molina, L. T. A possible pathway for rapid growth of sulfate during haze days in China. *Atmos. Chem. Phys.* **2017**, *17*, 3301–3316.
- (34) Tang, M.; Larish, W. A.; Fang, Y.; Gankanda, A.; Grassian, V. H. Heterogeneous Reactions of Acetic Acid with Oxide Surfaces: Effects of Mineralogy and Relative Humidity. *J. Phys. Chem. A* **2016**, *120*, 5609–16.
- (35) Underwood, G. M.; Song, C. H.; Phadnis, M.; Carmichael, G. R.; Grassian, V. H. Heterogeneous reactions of NO<sub>2</sub> and HNO<sub>3</sub> on oxides and mineral dust: A combined laboratory and modeling study. *J. Geophys. Res.* **2001**, *106*, 18055–18066.
- (36) Kebede, M. A.; Bish, D. L.; Losovyj, Y.; Engelhard, M. H.; Raff, J. D. The Role of Iron-Bearing Minerals in NO<sub>2</sub> to HONO Conversion on Soil Surfaces. *Environ. Sci. Technol.* **2016**, *50*, 8649–8660.
- (37) Fu, H.; Wang, X.; Wu, H.; Yin, Y.; Chen, J. Heterogeneous Uptake and Oxidation of SO<sub>2</sub> on Iron Oxides. *J. Phys. Chem. C* **2007**, *111*, 6077–6085.
- (38) Hixson, B. C.; Jordan, J. W.; Wagner, E. L.; Bevssek, H. M. Reaction products and kinetics of the reaction of NO<sub>2</sub> with gamma-Fe<sub>2</sub>O<sub>3</sub>. *J. Phys. Chem. A* **2011**, *115* (46), 13364–13369.
- (39) Baltrusaitis, J.; Schuttlefield, J.; Jensen, J. H.; Grassian, V. H. FTIR spectroscopy combined with quantum chemical calculations to investigate adsorbed nitrate on aluminium oxide surfaces in the presence and absence of co-adsorbed water. *Phys. Chem. Chem. Phys.* **2007**, *9*, 4970–4980.
- (40) Piazzesi, G.; Elsener, M.; Kröcher, O.; Wokaun, A. Influence of NO<sub>2</sub> on the hydrolysis of isocyanic acid over TiO<sub>2</sub>. *Appl. Catal., B* **2006**, *65*, 169–174.
- (41) Goodman, A. L.; Bernard, E. T.; Grassian, V. H. Spectroscopic Study of Nitric Acid and Water Adsorption on Oxide Particles: Enhanced Nitric Acid Uptake Kinetics in the Presence of Adsorbed Water. *J. Phys. Chem. A* **2001**, *105*, 6443–6457.
- (42) Underwood, G. M.; Miller, T. M.; Grassian, V. H. Transmission FT-IR and Knudsen Cell Study of the Heterogeneous Reactivity of Gaseous Nitrogen Dioxide on Mineral Oxide Particles. *J. Phys. Chem. A* **1999**, *103*, 6184–6190.
- (43) Wu, J.; Cheng, Y. In situ FTIR study of photocatalytic NO reaction on photocatalysts under UV irradiation. *J. Catal.* **2006**, *237*, 393–404.
- (44) Guan, C.; Li, X.; Luo, Y.; Huang, Z. Heterogeneous reaction of NO<sub>2</sub> on alpha-Al<sub>2</sub>O<sub>3</sub> in the dark and simulated sunlight. *J. Phys. Chem. A* **2014**, *118*, 6999–7006.
- (45) Sun, Z.; Kong, L.; Ding, X.; Du, C.; Zhao, X.; Chen, J.; Fu, H.; Yang, X.; Cheng, T. The effects of acetaldehyde, glyoxal and acetic acid on the heterogeneous reaction of nitrogen dioxide on gamma-alumina. *Phys. Chem. Chem. Phys.* **2016**, *18*, 9367–9376.
- (46) Szanyi, J.; Kwak, J. H.; Chimentao, R. J.; Peden, C. H. Effect of H<sub>2</sub>O on the Adsorption of NO<sub>2</sub> on gamma-Al<sub>2</sub>O<sub>3</sub>: an in Situ FTIR-MS Study. *J. Phys. Chem. C* **2007**, *111*, 2661–2669.
- (47) Li, H. J.; Zhu, T.; Zhao, D. F.; Zhang, Z. F.; Chen, Z. M. Kinetics and mechanisms of heterogeneous reaction of NO<sub>2</sub> on

CaCO<sub>3</sub> surfaces under dry and wet conditions. *Atmos. Chem. Phys.* **2010**, *10*, 463–474.

(48) Tan, F.; Tong, S.; Jing, B.; Hou, S.; Liu, Q.; Li, K.; Zhang, Y.; Ge, M. Heterogeneous reactions of NO<sub>2</sub> with CaCO<sub>3</sub>–(NH<sub>4</sub>)<sub>2</sub>SO<sub>4</sub> mixtures at different relative humidities. *Atmos. Chem. Phys.* **2016**, *16*, 8081–8093.

(49) Venkov, T.; Hadjiivanov, K.; Klissurski, D. IR spectroscopy study of NO adsorption and NO + O<sub>2</sub> co-adsorption on Al<sub>2</sub>O<sub>3</sub>. *Phys. Chem. Chem. Phys.* **2002**, *4*, 2443–2448.

(50) Zhang, L.; He, H. Mechanism of selective catalytic oxidation of ammonia to nitrogen over Ag/Al<sub>2</sub>O<sub>3</sub>. *J. Catal.* **2009**, *268*, 18–25.

(51) Yamazoe, S.; Okumura, T.; Hitomi, Y.; Shishido, T.; Tanaka, T. Mechanism of Photo-Oxidation of NH<sub>3</sub> over TiO<sub>2</sub>: Fourier Transform Infrared Study of the Intermediate Species. *J. Phys. Chem. C* **2007**, *111*, 11077–11085.

(52) Busca, G. FT-IR study of the surface chemistry of anatase-supported vanadium oxide monolayer catalysts. *Langmuir* **1986**, *2*, 577–582.

(53) Wu, Q.; Gao, H.; He, H. Conformational Analysis of Sulfate Species on Ag-Al<sub>2</sub>O<sub>3</sub> by Means of Theoretical and Experimental Vibration Spectra. *J. Phys. Chem. B* **2006**, *110*, 8320–8324.

(54) Huang, Z.; Zhang, Z.; Kong, W.; Feng, S.; Qiu, Y.; Tang, S.; Xia, C.; Ma, L.; Luo, M.; Xu, D. Synergistic effect among Cl<sub>2</sub>, SO<sub>2</sub> and NO<sub>2</sub> in their heterogeneous reactions on gamma-alumina. *Atmos. Environ.* **2017**, *166*, 403–411.

(55) Sugimoto, T.; Wang, Y. Mechanism of the Shape and Structure Control of Monodispersed α-Fe<sub>2</sub>O<sub>3</sub> Particles by Sulfate Ions. *J. Colloid Interface Sci.* **1998**, *207*, 137–149.

(56) Saur, O.; Bensitel, M.; Mohammed Saad, A. B.; Lavalley, J. C.; Tripp, C. P.; Morrow, B. A. The Structure and Stability of Sulfated Alumina and Titania. *J. Catal.* **1986**, *99*, 104–110.

(57) Goodman, A. L.; Li, P.; Usher, C. R.; Grassian, V. H. Heterogeneous Uptake of Sulfur Dioxide on Aluminum and Magnesium Oxide Particles. *J. Phys. Chem. A* **2001**, *105* (25), 6109–6120.

(58) Warschkow, O.; Ellis, D. E. Defects and Charge Transport near the Hematite (0001) Surface: An Atomistic Study of Oxygen Vacancies. *J. Am. Ceram. Soc.* **2002**, *85*, 213–220.

(59) Al-Abadleh, H. A.; Grassian, V. H. FT-IR Study of Water Adsorption on Aluminum Oxide Surfaces. *Langmuir* **2003**, *19*, 341–347.

(60) Ishikawa, T.; Cai, W. Y.; Kandori, K. Adsorption of Molecules onto Microporous Hematite. *Langmuir* **1993**, *9*, 1125–1128.

(61) Beale, A. M.; Gao, F.; Lezcano-Gonzalez, I.; Peden, C. H.; Szanyi, J. Recent advances in automotive catalysis for NOx emission control by small-pore microporous materials. *Chem. Soc. Rev.* **2015**, *44*, 7371–7405.

(62) Baltrusaitis, J.; Cwiertny, D. M.; Grassian, V. H. Adsorption of sulfur dioxide on hematite and goethite particle surfaces. *Phys. Chem. Chem. Phys.* **2007**, *9*, 5542–5554.

(63) Xie, Y.; Chen, Y.; Ma, Y.; Jin, Z. Investigation of simultaneous adsorption of SO<sub>2</sub> and NO on gamma-alumina at low temperature using DRIFTS. *J. Hazard. Mater.* **2011**, *195*, 223–229.

(64) Ishizuka, T.; et al. Initial Step of Flue Gas Desulfurizations - An IR Study of the Reaction of SO<sub>2</sub> with NOx on CaO-. *Environ. Sci. Technol.* **2000**, *34*, 2799–2803.

(65) Pinder, R. W.; Adams, P. J. Ammonia Emission Controls as a Cost-Effective Strategy for Reducing Atmospheric Particulate Matter in the Eastern United States. *Environ. Sci. Technol.* **2007**, *41*, 380–386.

(66) Sun, Y.; Jiang, Q.; Wang, Z.; Fu, P.; Li, J.; Yang, T.; Yin, Y. Investigation of the sources and evolution processes of severe haze pollution in Beijing in January 2013. *J. Geophys. Res.* **2014**, *119*, 4380–4398.